Front. Earth Sci. China 2009, 3(4): 471–479
DOI 10.1007/s11707-009-0064-y

RESEARCH ARTICLE

Centennial fluctuations of flood-season discharge of Upper and Middle Yangtze River Basin, China (1865–1988): cause and impact

Yonghong DONG (✉)[1], Zhanghua WANG[2], Zhongyuan CHEN[2], Daowei YIN[2]

1 Department of Geography, East China Normal University, Shanghai 200062, China
2 State Key Laboratory for Estuarine and Coastal Research, East China Normal University, Shanghai 200062, China

Abstract This paper reveals the nature of flood-season discharge and the associated impact on the upper and middle Yangtze river basin, on the basis of a historical database of daily discharges recorded at the Yichang (1865–1985) and Hankou (1878–1988) hydrological stations. Results show the period of discharge fluctuations of 2–6a, which is significant during 1878–1900 and 1915–1975 at Yichang station and the period of 2–7a during 1865–1905 and 1925–1975 at Hankou station. Within these periods, a major period of 2.9–3.5a and two secondary periods of 7–8a and 13.9–16.5a can be further identified from both stations. Our observation verifies that the fluctuations of streamflows of the upper and middle Yangtze River are fairly consistent with the periodicities of the Asia monsoon precipitation and ENSO event, reflecting coupling effect on the fluctuations of discharges in the Yangtze basin. In the 1920s–1960s, intensified variability of streamflows of the upper and middle Yangtze River was closely associated with warming temperature in the basin and in China as well. In 1975–1988, insignificant discharge fluctuations recorded at both stations can be chiefly attributed to human activities, i.e., the large number of reservoirs constructed and associated increasing capacity of water storage, which has largely weakened the discharge fluctuations throughout the basin.

Keywords discharge fluctuations, period of discharge, Yangtze runoff, hydro-climate linkage

1 Introduction

As an important part of water circulation, river discharges are most vital for sustainable development, utilization of water resources and better governance. Water modification depends not only on the effect of global climate change, but also on human activities, both affecting our societal development in recent years (Zhang et al., 2006). In the past decades, runoff distribution in relation to climate change has become an increasing concern. Inter-annual and inter-decadal fluctuations of discharge are well documented at different scales. These fluctuations have been emphasized by the analysis of atmospheric disturbances, such as sea-level pressure, sea surface temperature (SST) and continental surface temperature oscillations (Labat, 2008). Indeed, fluvial hydrological signals can bring sensitive information about climate fluctuations (Zhang et al., 2008). Kondrashov et al. (2005) examined the periods of the Nile river-water level (622–1922), revealing that the short period of water-level oscillatory can correlate the ENSO event and the North-Atlantic influences, but the long period might be of astronomical origin. Labat (2008) tested the variance of the main rivers of the world during the 19th–20th centuries, finding that kinship exits between the land water cycle oscillations and climate forcing. This relationship has been also established in many researches in China (seeing Lan et al., 2002). In general, a dry year often occurs with an El Nino event, while a flood year with a La Nina event (Lan et al., 2002).

The Yangtze River is the longest river in China and the third longest in the world. It lies between 91°E and 122°E, and 25°N and 35°N and plays a vital role in promoting economic development in China. The river originates in the Qinghai-Tibet Plateau, flows about 6300 km eastwards to the East China Sea, and forms a drainage basin of about

Received April 28, 2009; accepted August 7, 2009

E-mail: Dongyonghong2004@163.com

1800000 km^2 (Zhang et al., 2006). Monsoon precipitation prevails in the Yangtze River basin, where there is a mean annual precipitation of about 1100 mm and a mean annual freshwater discharge of ~934 billion m^3 into the seas. Runoff in the upper Yangtze reach comes primarily from the Indian summer monsoon precipitation and the one in the middle and lower Yangtze reaches is mainly derived from the East Asian summer monsoon (Ding and Chan, 2005; Zhang et al., 2006, 2007). The variability of runoff of the basin is closely coupled to atmospheric teleconnection, such as the El Niño–ENSO oscillations.

Many previous studies were performed on the streamflows and climate changes of the Yangtze River basin. Yang et al. (2005) established significant relationship between precipitation and runoff by least squares method. Zhang et al. (2005a) analyzed the monthly precipitation, temperature and runoff from 1950 to 2002. Their results indicate the upward trend of precipitation in the middle and lower Yangtze basin, but downward trend and upward trend in the upper Yangtze basin. Xu et al. (2006) examined the long-term variation tendency of precipitation and runoff in the Yangtze River basin, indicating that the trend of change in runoff is basically consistent with the trend of change in precipitation. Other studies have further revealed the Yangtze floods and droughts in relation to teleconnections with ENSO activities (1470–2003), showing the significant correlation between ENSO and flood/drought (Jiang et al., 2006). There is a variability and teleconnection between annual maximum streamflow in the Yangtze River basin and El Niño/ENSO (Zhang et al., 2007). Different phases of relations were corroborated between the annual maximum streamflow of the Yangtze River basin and ENSO. In-phase relationship occurs in the lower Yangtze River and an anti-phase relationship appears in the upper Yangtze River, but an ambiguous phase exists in the middle Yangtze River, implying a hydro-climate transition zone in the middle Yangtze River basin (Zhang et al., 2007).

The Yangtze River basin has been strongly affected by human activities, in particular, the construction of reservoirs and inter-basin water transfer, which have exerted a great impact on the distribution of runoff. For example, there was an approximately 15-year period of discharge fluctuation, both recorded at the Yichang (1882–2000) and Hankou hydrological gauging station (1870—2000), but this periodicity has been obviously destroyed since 1970, primarily due to strong human interferences on the basin surface (Wang et al., 2006). The variability of precipitation in the Yangtze River basin seems agreeable with global climate warming and climate instability, which has intensifies drought and flood events recently (Zhang et al., 2008). Under such circumstances, what kind of new features in runoff of the Yangtze River basin will appear becomes a question that draws our attention.

Geophysical time series is often generated by complex systems, which we know little about. Predictable behavior in such systems, such as trends and periodicities, is therefore of great interest. Most traditional mathematical methods that examine periodicities in the frequency domain, such as Fourier analysis, seem only suitable for stationary time series, although it is of positioning frequency accuracy. However, many phenomena on the earth's surface, such as streamflows, earthquake wave, storms, floods, etc., are affected by multiple factors, of which most are unsmooth sequence, not only having characteristics of tendency and periodicity, but also of structures of random, sudden and multi-time nature (Wang et al., 2002).

The factors follow a multi-level evolving principle. Wavelet transform analysis has a time-frequency function, which provides possibility for better researches on time sequence. Wavelet transform can reveal hidden change periods in a variety of time-series, to reflect changing trend of the system with different time scales. Recently, wavelet analysis has become a common tool for analyzing localized variations of power within a time series (Torrence and Compo, 1998, Grinsted et al., 2004). The Morlet wavelet analysis of the hydrological time series makes it possible to study temporal oscillations and major periods; therefore, it has been widely applied to the study of streamflow changes of rivers, including the Yangtze River in China (Wang et al., 2002; Zhang et al., 2006, 2007; Labat, 2008). The present study selects the Morlet continuous wavelet transform (CWT) to examine the hydrological time series at the Yichang and Hankou stations (flood season) and thus to be able to identify temporal oscillations and major periods with different time scales.

In short, the main objectives of the present study are: 1) to investigate temporal runoff oscillations and associated major periods at the two hydrological gauging stations (Yichang and Hankou station, Fig. 1) in the Yangtze River; 2) to analyze the mechanism that drives the period of discharge fluctuations in association with climate change; and 3) to better understand the effect of alternated hydrology due to human interferences.

2 Data and methods

2.1 Data

The runoff data of the yearly flood season (6–10 month) were collected from two hydrological gauge stations of the Yangtze River basin (Changjiang Water Resources Commission, 1865–1988): Yichang station and Hankou station. The time series data at the two stations are 1877–1988 and 1865–1985, respectively. We use the standardized data in this paper (Fig. 2).

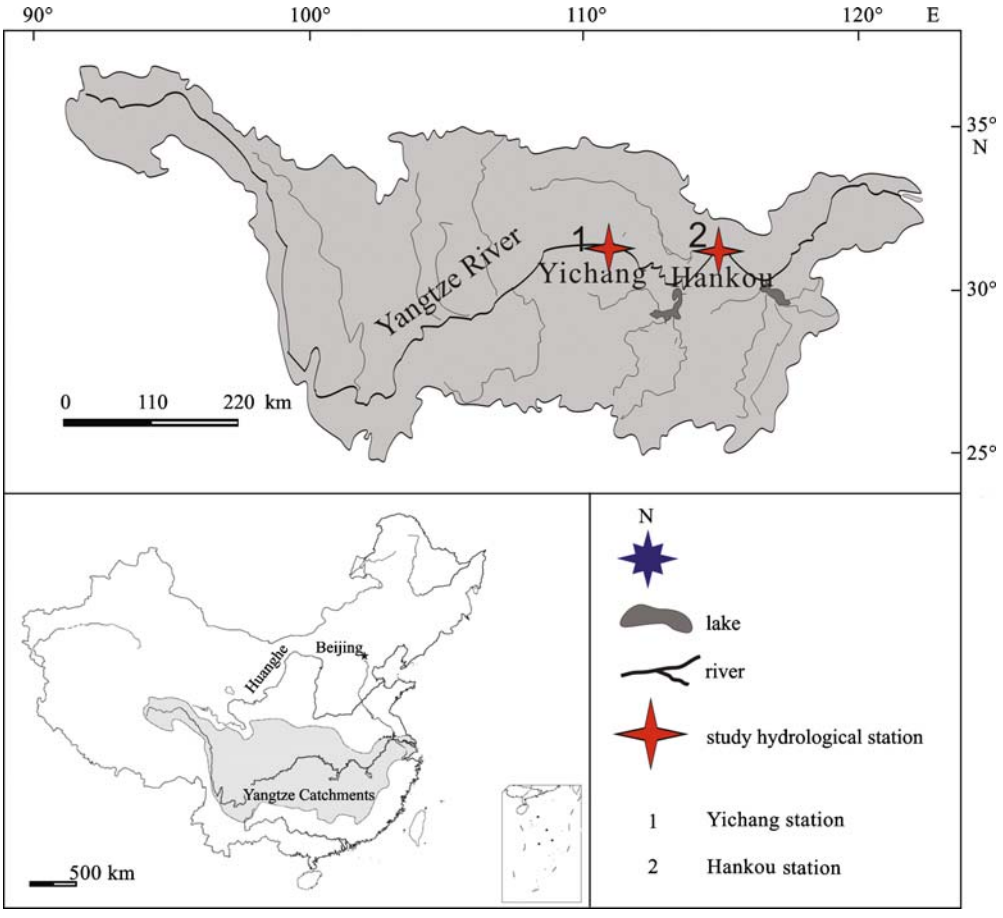

Fig. 1 Geographic location of the Yangtze River basin, where Yichang and Hankou hydrological stations are marked

2.2 Methods

The standardized method for raw data of discharge is defined as

$$R' = \frac{R-\overline{R}}{\sigma},$$

where R is raw data or measured data of discharge, $\overline{R}$ is average of R. σ is standard deviation for R.

The continuous wavelet transform (CWT) (Torrence and Compo, 1998) is used in this study, assuming that x_n is a time series with equal time spacing δt and $n=0,\ldots,N-1$. We also assume that one has a wavelet function $\psi_0(\eta)$ that depends on a nondimensional "time" parameter η. To be "admissible" as a wavelet, this function must have zero mean and be localized in both time and frequency space (Torrence and Compo, 1998). Because Morlet wavelet provides a good balance between time and frequency localization, we applied the Morlet wavelet, which is defined as:

$$\psi_0(\eta) = \pi^{-1/4} e^{i\omega_0\eta} e^{-\eta^2/2}, \quad (1)$$

where ω_0 is the nondimensional frequency, here taken to be 6 to satisfy the admissibility condition (Torrence and Compo, 1998). The CWT of a discrete sequence x_n is defined as the convolution of x_n with a scaled and translated version of $\psi_0(\eta)$:

$$W_n(s) = \sum_{n'}^{N-1} x_{n'} \psi^* \left[\frac{(n'-n)\delta t}{s}\right], \quad (2)$$

where the (*) indicates the complex conjugate. We define the wavelet power as $|W_n(s)|^2$.

The CWT has edge artifacts because the wavelet is not completely localized in time. It is therefore useful to introduce a Cone of Influence (COI) in which edge effects cannot be ignored. Here we take the COI as the area in which the wavelet power caused by a discontinuity at the edge has dropped to e^2 of the value at the edge (Torrence and Compo, 1998). The statistical significance of wavelet power can be assessed under the null hypothesis that the signal is generated by a stationary process being given the background power spectrum (P_k). It is assumed that the time series has a mean power spectrum, possibly given by (3); if a peak in the wavelet power spectrum is significantly above this background spectrum, then it can be assumed to be a true feature with a certain percent confidence. The

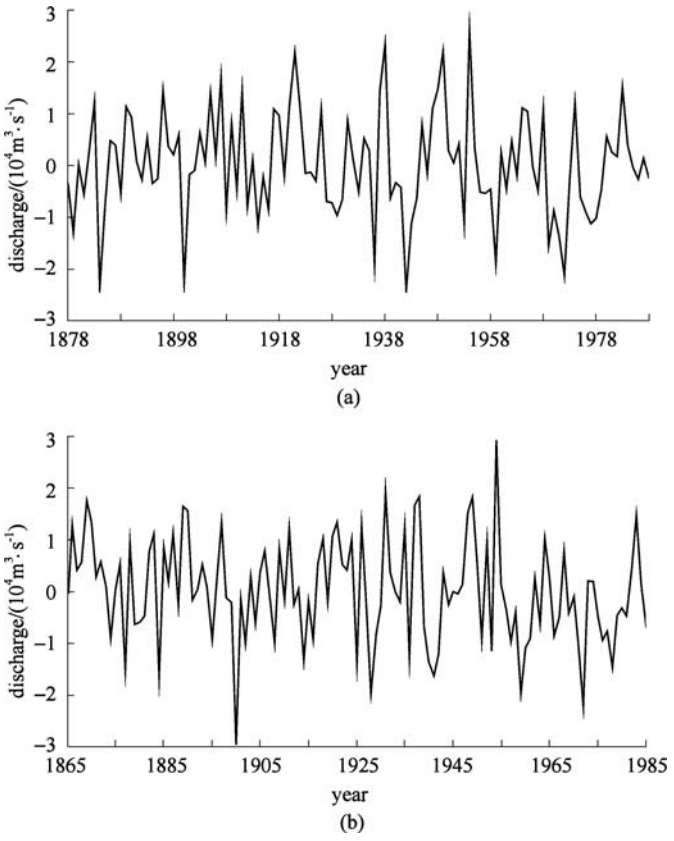

Fig. 2 Standardized yearly discharge of flood season at Yichang station (a) and Hankou station (b)

"95% confidence interval" refers to the range of confidence about a given value. To determine the 95% confidence level (significant at 5%), one multiplies the background spectrum (3) by the 95th percentile value for χ^2 (Torrence and Compo, 1998). Many geophysical series have the red noise characteristics which can be modeled by a first order autoregressive (AR(1)) process. The Fourier power spectrum of an AR (1) process with lag-1 autocorrelation α is given by (Grinsted et al., 2004) as

$$P_K = \frac{1-\alpha^2}{\left|1-\alpha e^{-2i\pi K}\right|^2}, \tag{3}$$

where k is the Fourier frequency index. Torrence and Compo (1998) used the Monte Carlo method to show that the probability that the wavelet power of a process with a given power spectrum (P_k) is greater than p is

$$D\left(\frac{\left|W_n^X(s)\right|^2}{\sigma_X^2} < p\right) = \frac{1}{2}P_K\chi_v^2(P), \tag{4}$$

where v is equal to 1 for real and 2 for complex wavelets. When $|W_n(s)|^2 > p$, wavelet power spectrum is significant.

Global wavelet spectrum shows the different scales of the energy density, which is defined as

$$\overline{W}^2(s) = \frac{1}{N}\sum_{n=0}^{N-1}|W_n(s)|^2, \tag{5}$$

the given global power spectrum is $P = \sigma_X^2 P_k * \frac{x_v^2}{v}$, $\alpha = 0.05$, where x_v^2 is the chi-square distribution with v degrees of freedom, $v = 2\sqrt{1+\frac{N\delta t}{2.32s}}$. When $\overline{W}^2(s) > p$, the global wavelet spectrum corresponding to the period is significant.

Scale-averaged power spectrum examines fluctuations in power over a range of scale (a band), which is defined as

$$\overline{W}_n^2 = \frac{\delta_j * \delta_t}{0.776}\sum_{j=j_1}^{j_2}\frac{\left|W_n(s_j)\right|^2}{s_j}, \tag{6}$$

the given scale-averaged power spectrum is $P = \frac{\sigma_X^2\delta_j\delta_t\overline{P}}{0.776^* S_{avg}} * \frac{x_v^2}{v}$, $\alpha = 0.05$, where x_v^2 is the chi-square distribution with v degrees of freedom,

$$v = \frac{2(j_2 - j_1 + 1)^* S_{avg}}{S_{mid}} * \sqrt{1 + \left(\frac{(j_2 - j_1 + 1)^*\delta_j}{0.6}\right)^2},$$

$$S_{avg} = \sum_{j=j_1}^{j_2} \frac{1}{s_j}, \quad S_{mid} = S_0{}^* 2^{0.5(j_2+j_1)\delta_j}, \quad \overline{P} = s_{avg} * \sum_{j=j_1}^{j_2} \frac{P_{s_j}}{s_j}.$$

When $\overline{W}_n^2 > P$, the scale-averaged power spectrum is significant.

According to Torrence and Compo (1998), the relationship between Morlet wavelet scale (s) and period (T) is defined as

$$T = \frac{4\pi s}{w_0 + \sqrt{2 + w_0^2}} = 1.033s \ (w_0 = 6).$$

3 Results

The continuous wavelet power spectra for standardized yearly discharges of the flood season at both stations are depicted in Fig. 3. This shows different scales and time periods for the time series database. High wavelet power spectrum reveals the period of discharge fluctuations of 2–6a (dominated by 3–4a oscillation) at Yichang station for the time of 1878–1900 and 1915–1975 (Fig. 3(a)). High wavelet power spectrum also occurs at Hankou station, with 2–7a period (dominated by 3–4a oscillation) for 1865–1905 and 1925–1975 (Fig. 3(b)). In addition, there is obviously a period of 14–17a recorded at both stations, but it does not pass through the test of 95% confidence level.

In order to further determine the major periods of streamflow along with time, it is worthy to understand the global wavelet spectrum and scale-averaged wavelet power (Figs. 4 and 5(a)). Using global wavelet spectrum can highlight 2–6a discharge fluctuation at Yichang station, and 2–7a at Hankou station (both significant at >95% confidence level). During these time periods, the major period at both stations is 2.9–3.5a (Fig. 4). Of note, there are periods of 13.9a and 8.3a at Yichang station and 16.5a and 6.9a at Hankou station, with a higher wavelet

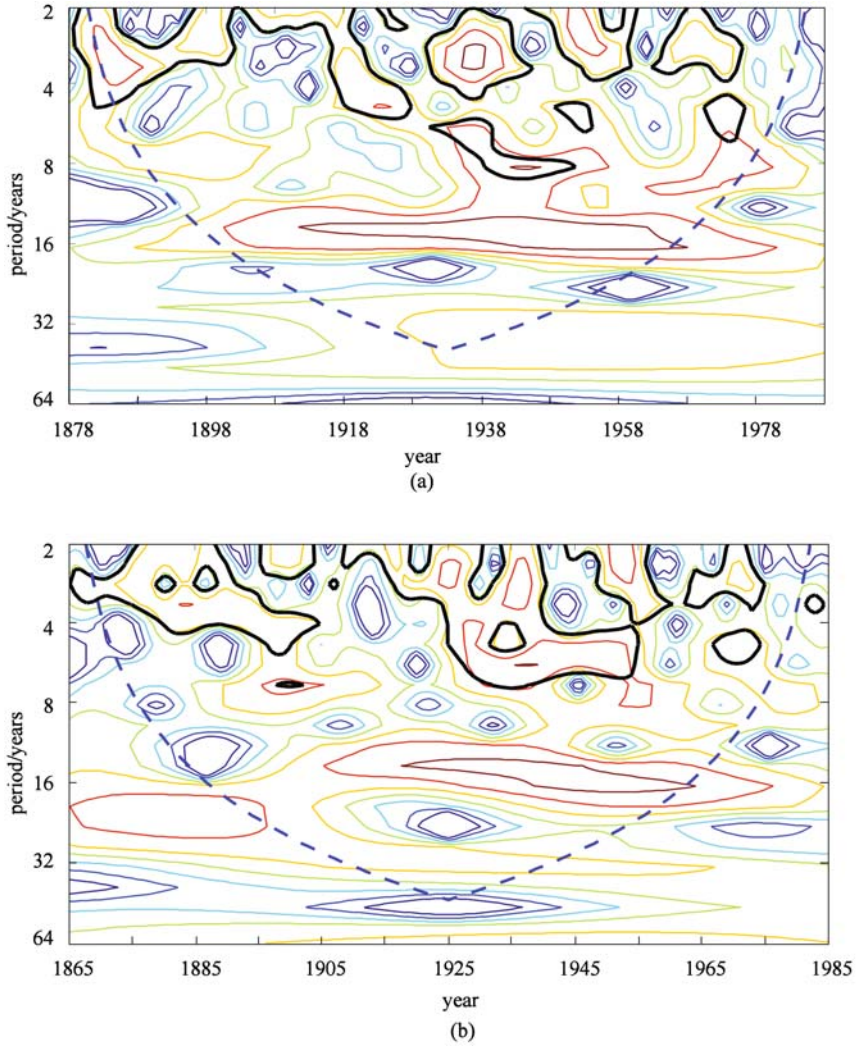

Fig. 3 Wavelet power spectrum of standardized yearly discharge of flood season at (a) Yichang station and (b) Hankou station. Dashed U-shaped line indicates the Cone of Influence (COI) region. Thick solid line represents the periods significant at >95% confidence level

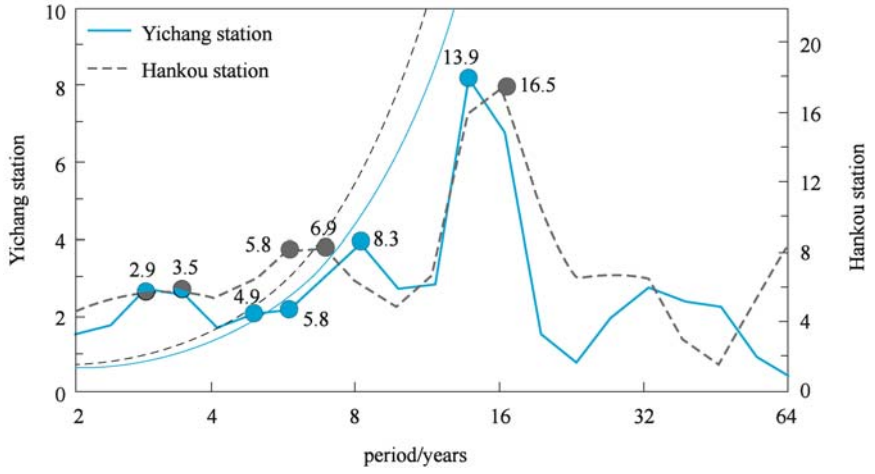

Fig. 4 Global wavelet spectrum of standardized yearly flood season discharge at Yichang station (blue solid) and Hankou station (black dashed), respectively. Thin blue solid line stands for 95% confidence level for Yichang station, and thin black dashed line stands for 95% level for Hankou station.

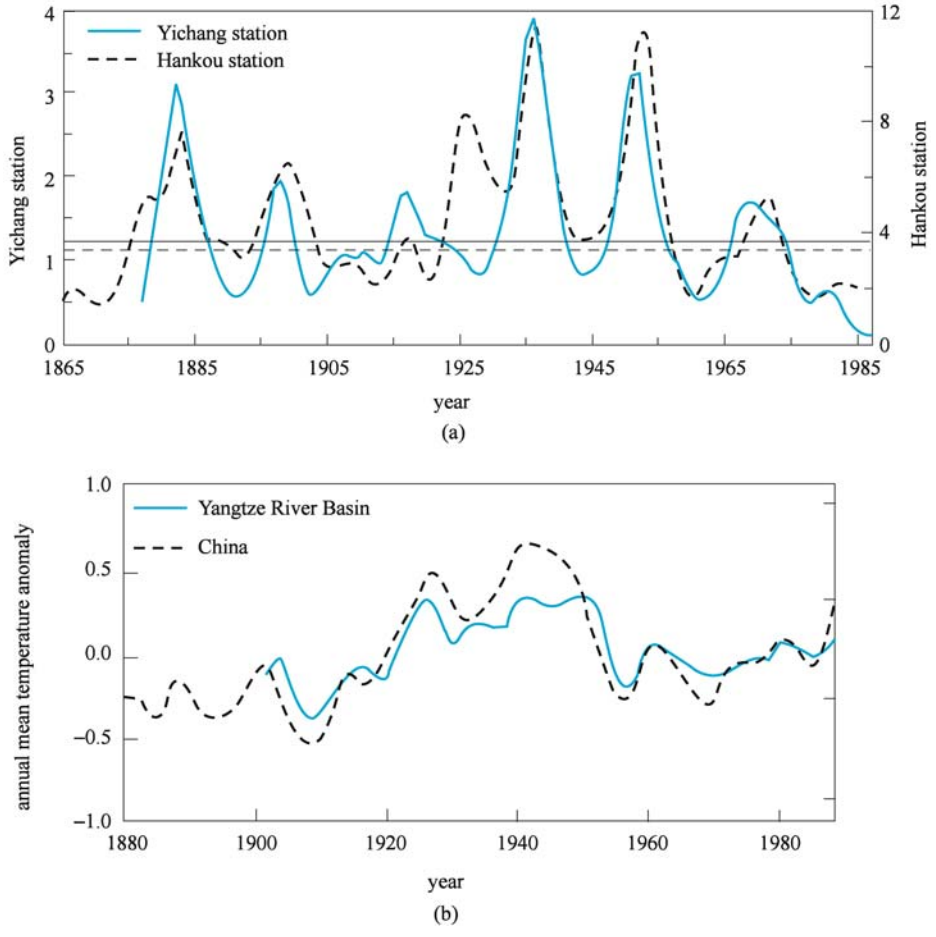

Fig. 5 (a) 2–6a and 2–7a scale-averaged power spectrum of standardized yearly discharge of flood season at Yichang station (blue solid) and Hankou station (black dashed), respectively. Thin blue solid line stands for 95% confidence level for Yichang station, and thin black dashed line represents 95% level for Hankou station; (b) annual mean temperature anomaly in the Yangtze River basin (1900–1988) and China (1880–1988) (modified after Wang et al., 2001; He et al., 2007)

power, but these are insignificant at >95% confidence level. Scale-averaged wavelet power shows the similar features of over 2–6a band at Yichang station and 2–7a band at Hankou station (Fig. 5(a)). The variance plot shows two distinct periods during 1878–1900 and 1915–1975 when the discharge variance is significant at Yichang station (Fig. 5(a)). This is also significant for the time period of 1865–1905 and 1925–1975 at Hankou station (Fig. 5(a)). Both time series show consistent inter-decadal changes of 14–17a period.

4 Discussion

With the help of CWT analysis, 2–6a period of discharge time series at Yichang station (flood season) is remarkable, as well as 2–7a at Hankou station (Figs. 3 and 4). During these periods, there appears a dominant period of 2.9–3.5a in the flood season. Also there exist secondary periods of 7–8a and 13.9–16.5a (Fig. 4). Tan et al. (1993) analyzed the annual discharge at Yichang station (1882–1986), which comes to the conclusion of 14–15a period. Pavla et al. (2003) examined the yearly streamflow at Hankou station (1865–1986), revealing that discharge fluctuation is characterized by the period of 7a and 14a. Wang et al. (2006) revealed monthly discharges with 15a and quasi-7a period, both at the Yichang station (1882–2000) and Hankou station (1870–2000). Zhang et al. (2005b) and Zhang et al. (2006) found changing trends of water level in the past 130 years, demonstrating that both Yichang (1877–2000) and Hankou station (1865–2000) are dominated by the period of 3–4a and 7–8a. Wang et al. (2002) explained the 15a, 8–9a and 3–4a periods of annual discharge fluctuations at Yichang station (1890–1987). However, these have almost not been tested for confidence level, leading to some uncertainties of the main oscillations of streamflows.

Because of the lack of long-term runoff time series at Datong station of the lower Yangtze, here we do not attempt the trend of evolution of its period. However, Yang et al. (2005) found that the relationship of yearly discharge between Datong and Hankou stations (1865–2004) is significant (>95 % confidence level). What is more, Wang et al. (2006) used the periodogram and maximum entropy spectrum to study the annual discharge at Datong station and the result shows 6–7a and 15–16a period of discharge fluctuations.

The upper Yangtze River is primarily influenced by the Indian summer monsoon and the middle and lower Yangtze River is overwhelmed by the East Asian summer monsoon (Ding and Chan, 2005). Both are independent, but interact with each other (Ding and Chan, 2005). These two climatic systems are not in synchronization spatially and temporally, leading to different changing trends of precipitation in the upper, middle and lower Yangtze basin (Zhang, et al., 2005b). The Yichang and Hankou stations are very important sites for representing the upper and middle Yangtze River. Therefore, the major periods of the two stations can represent the trend of precipitation change in southwestern China, including the middle and lower Yangtze basin. In other words, the periods of discharge at both stations can reflect the fluctuations of the Asia monsoon to some extent.

ENSO event has a period of 2–7a with a dominant period of 3–4a (Torrence and Compo, 1998). Although many researchers have indicated that ENSO only occurs in the equatorial Pacific, it can influence regional climate settings in regions covering more than 75% of the earth (Long and Li, 1999). Wang et al. (2000) have found that an ENSO event can modify the East Asian climate through a Pacific-East Asian (PEA) teleconnection. The occurrence of ENSO generally reinforces the connection between the South Asian summer monsoon and the East Asian summer rainfall variations (Hu et al., 2005). There is a relationship between ENSO and the annual maximum streamflow of the Yangtze River, showing 2–4a period during 1890–1900 and 8–16a period during 1920–1930 (Zhang et al., 2007). Such relationship also exists in Yichang station with 2–8a period during 1875–1882 and 1960–1980 in Hankou station. In our study, 2–6a period of discharge time series at Yichang station and 2–7a at Hankou station (flood season) might have a close linkage to the 2–7a period of the ENSO event and the major period 2.9–3.5a could be associated with 3–4a of ENSO. There also exists a 15a period of ENSO variance (Torrence and Compo, 1998), which may influence a 13.9–16.5a period of discharge at both stations. Therefore, we believe that the effect of ENSO and the Asia monsoon adds more influence on the period of discharge fluctuations of the Yangtze basin.

Another prominent phenomenon is seen from scale-averaged power spectrum. We found that 2–6a period of discharge time series at Yichang station and 2–7a at Hankou station (1920s–1960s) is significant (Fig. 5(a)), but, ENSO has low variation during this time period (Torrence and Compo, 1998). Therefore, the obvious fluctuation of discharge at both stations is not necessarily linked to ENSO. Previous researches show that a change of temperature would change the trend of runoff fluctuations (Labat et al., 2004). The average temperature in China has the quasi-15a and 28a period of inter-decadal scale, and quasi-2–3a and quasi-8–9a of inter-annual scale in the past 100 years, of which the major period is quasi-2–3a (Yu et al, 2000). Quasi-4a period of temperature along the middle and lower Yangtze River is remarkable (Zhu et al, 2003). Therefore, discharges at Yichang and Hankou station are most likely driven by the oscillations of temperature. We know that inter-decadal high temperature occurred in the Yangtze River valley during the 1920s–1960s (Fig. 5 (b)) (Wang et al., 2001; He et al., 2007), which could intensify the variability of streamflows of the Yangtze River.

There was no significant fluctuations at both stations

after 1975 (Figs. 3 and 4 (a)), although the variance of ENSO prevailed. We believe that this can be attributed to intensifying human activities (Yin and Li, 2001). During the 1960s–1970s, large-scale water conservancy projects started in the main tributaries of the Yangtze basin. Water impoundments have increased the capacity of water storage of greater than 13.5 billion m^3/s, which plays a great role in regulating runoff in the middle and lower Yangtze reaches (Xu et al., 2006; Li et al., 2007). As result, variation of streamflow has attenuated and consequently, weakened the period of discharge oscillations.

5 Conclusions

The Morlet continuous wavelet analysis is powerful tool for identifying temporal discharge fluctuations with major periods of discharge fluctuations. The time series of flood-season discharges recorded at Yichang (1865–1985) and Hankou station (1878–1988) of the upper and middle Yangtze River basin were analyzed by CWT. We conclude below.

At Yichang station, the period of 2–6a is significant during 1878–1900 and 1915–1975, while the period of 2–7a occurs during 1865–1905 and 1925–1975 at Hankou station. However, during these time periods, there exist a major period of 2.9–3.5a and secondary periods of 7–8a and 13.9–16.5a, which can be further identified from both stations.

The fluctuations of streamflows keep fairly in an agreement with the periodicities of the Asia monsoon precipitation and ENSO events, reflecting their coupling effect that influence the discharge fluctuations in the Yangtze River basin. The periods of discharge at both stations are believed to be closely associated with the fluctuations of the Asia monsoon and ENSO event.

From the 1920s to 1960s, the variability of streamflows was probably driven by warming temperature that occurred in the upper and middle of the Yangtze River. After the mid-1970s, the large number of reservoir construction would have weakened the oscillations of discharge.

Acknowledgements We thanked Christopher Torrence and Gilbert P. Compo, who provided the wavelet software: http://paos.colorado.edu/research/wavelets.

References

Changjiang Water Resources Commission (Ministry of Water Resources, China) (CWRC), (1865–1988). Hydrological Records of the Yangtze River. Beijing: Cyclopedia Press of China (in Chinese)

Ding Y H, Chan J C L (2005). The East Asian summer monsoon: an overview. Meteorology and Atmospheric Physics, 89: 117–142

Grinsted A, Moore J C, Jevrejeva S (2004). Application of the cross wavelet transform and wavelet coherence to geophysical time series. Nonlinear Processes in Geophysics, 11: 561–566

He L, Wu Y J, Dan C J, Xue H P (2007). Impacts of global temperature changes in last century on drought and flood disasters in Yangtze River Basin. Chinese Journal of Agrometeorology, 28(4): 364–366 (in Chinese)

Hu Z Z, Wu R G, Kinter J L, et al (2005). Connection of summer rainfall variations in South and East Asia: role of El Niño-southern oscillation. International Journal of Climatology, 25: 1279–1289

Jiang T, Zhang Q, Zhu D M, Wu Y J (2006). Yangtze floods and droughts (China) and teleconnections with ENSO activities (1470–2003). Quaternary International, 144 (1): 29–37

Kondrashov D, Feliks Y, Ghil M (2005). Oscillatory modes of extended Nile River records (A.D. 622-1922). Geophysical Research Letters, 32: doi:10.1029/2004GL022156

Labat D (2008). Wavelet analysis of the annual discharge records of the world's largest rivers. Advances in Water Resources, 31: 109–117

Labat D, Godderis Y, Probst J L, Guyot J L (2004). Evidence for global runoff increase related to climate warming. Advance in Water Resources, 27: 631–642

Lan Y C, Ma Q J, Kang E, Zhang J S, Zhang Z H (2002). Relationship between ENSO cycle and abundant or low runoff in the upper Yellow River (China). Journal of Desert Research, 22(3): 262–266 (in Chinese)

Li M T, Xu K Q, Watanabe M, Cheng Z Y (2007). Long-term variations in dissolved silicate, nitrogen, and phosphorus flux from the Yangtze River into the East China Sea and impacts on estuarine ecosystem. Estuarine, Coastal and Shelf Science, 71: 3–12

Long Z X, Li C Y (1999). GCM modeling of the impacts of the ENSO on East Asian Monsoon activities. Acta Meteorologica Sinica, 57(6): 663–671 (in Chinese)

Pavla P, Pavol M, Jan P (2003). Spatial and temporal runoff oscillation analysis of the main rivers of the world during the 19th–20th centuries. Journal of Hydrology, 274: 62–79

Tan A J, Chen X Y, Zheng Y X (1993). Yichang runoff time series statistical analysis. Hydrology, 5: 15–21 (in Chinese)

Torrence C, Compo G P (1998). A practical guide to wavelet analysis. Bulletin of American Meteorological Society, 79: 61–78

Wang B, Wu R, Fu X (2000). Pacific-East Asian teleconnection: How does ENSO affect East Asian Climate?Journal of Climate, 13: 1517–1536

Wang G J, Jiang T, Chen G Y (2006). Structure and long-term memory of discharge series in Yangtze River. Acta Geographica Sinica, 61(1): 48–56 (in Chinese)

Wang S W, Gong D Y, Zhu J H (2001). Twentieth-century climatic warming in China in the context of the Holocene. The Holocene, 1: 313–321

Wang W S, Ding J, Li Y Q (2002). Hydrology wavelet analysis. Beijing: Chemical Industry Press (in Chinese)

Xu J J, Yang D W, Lei Z D, Li C, Peng J (2006). Examination on long time variation tendency of precipitation and runoff in the Yangtze River basin. Yangtze River, 37(9): 63–67 (in Chinese)

Yang S L, Gao A, Hotz H M, Zhu J, Dai S B, Li M (2005). Trends in annual discharge from the Yangtze River to the sea (1865–2004). Hydrological Sciences–Journal–des Sciences Hydrologiques, 50(5): 825–836

Yin H F, Li C A (2001). Human impact on floods and flood disasters on

the Yangtze River. Geomorphology, 41: 105–109

Yu J H, Ding Y G, Jiang Z H (2000). Singular spectrum analysis of temperature variations in China during the recent 100 years. Journal of Nanjing Institute of Meteorology, 23(4): 587–593 (in Chinese)

Zhang Q, Jiang T, Gemmer M, Becker S (2005a). Precipitation, temperature and discharge analysis from 1951 to 2002 in the Yangtze Catchments, China. Hydrological Sciences Journal, 50(1): 65–80

Zhang Q, Jiang T, Liu C L (2005b). Changing Trends of Water Level and Runoff during Past 100 Years of the Yangtze River (China). Asian Water, Environment and Pollution, 3(1): 49–55

Zhang Q, Liu C L, Xu C Y, Jiang T (2006). Observed trends of annual maximum water level and streamflow during past 130 years in the Yangtze River basin, China. Journal of Hydrology, 324: 255–265

Zhang Q, Xu C Y, Jiang T, Wu Y J (2007). Possible influence of ENSO on annual maximum streamflow of the Yangtze River, China. Journal of Hydrology, 333: 265– 274

Zhang Q, Xu C Y, Zhang Z X, Chen Y D, Liu C L, Lin H (2008). Spatial and temporal variability of precipitation maxima during 1960-2005 in the Yangtze River basin and possible association with large-scale circulation. Journal of Hydrology, 353: 215–227

Zhu Y F, Chen L X, Yu R C (2003). Analysis of the relationship between the China anomalous climate variation and ENSO cycle on the Quasi-four year scale. Journal of Tropical Meteorology, 19(4): 345–356 (in Chinese)